Thermochimica Acta 496 (2009) 38–44

Contents lists available at ScienceDirect

Thermochimica Acta

journal homepage: www.elsevier.com/locate/tca

Thermal behaviour, phase transition and molecular motions in $[Co(NH_3)_6](NO_3)_2$

Marta Liszka-Skoczylas, Edward Mikuli, Janusz Szklarzewicz, Joanna Hetmańczyk*

Jagiellonian University, Faculty of Chemistry, Ingardena 3, 30-060 Kraków, Poland

ARTICLE INFO

Article history:
Received 27 March 2009
Received in revised form 3 June 2009
Accepted 16 June 2009
Available online 25 June 2009

Keywords:
Hexaamminecobalt(II) nitrate(V)
Phase transition
Molecular reorientations
Thermal decomposition (TG/DTG/QMS)
Differential scanning calorimetry (DSC)
FT-IR
FT-RS and UV–vis spectra
X-ray powder diffraction (XRPD)

ABSTRACT

At room temperature $[Co(NH_3)_6](NO_3)_2$ possesses a regular (cubic) crystal lattice structure (space group $Fm\bar{3}m$) with the lattice parameter $a = 11.0441$ Å and with four molecules in the unit cell. One phase transition between 93 and 297 K, namely: at $T_C^h = 229.7$ K (during heating) and at $T_C^c = 225.2$ K (during cooling) was detected by differential scanning calorimetry. The presence of 4.5 K hysteresis suggests that the detected phase transition is of the first-order type. The splitting of the band connected with the $\nu_4(NO_3^-)E$ mode near the phase transition temperature T_C^c suggests lowering of the crystal lattice symmetry. The lack of a sudden change in temperature dependence of the FWHM of the band connected with the $\rho_w(NH_3)F_{1u}$ mode suggests that the phase transition is not connected with a fundamental change in the speed of NH_3 reorientational motions. The NH_3 ligands reorientate fast (correlation times equal to ca. several picoseconds) in both phases with an activation energy equal to ca. 11 kJ mol^{-1}. Thermal decomposition of the compound proceeds in two main stages. In the first stage, deammination of $[Co(NH_3)_6](NO_3)_2$ to $[Co(NH_3)_2](NO_3)_2$ takes place in two steps and four out of six NH_3 molecules per formula unit are liberated. The second stage is connected with the liberation of two residual NH_3 molecules and with the simultaneous decomposition of the resulting $Co(NO_3)_2$, leading to the formation of gaseous products of the decomposition (O_2, H_2O, N_2, nitrogen oxides) and solid CoO.

1. Introduction

The presence of ionic coordination compounds of the type: $[M(NH_3)_6]X_2$, where M = Ni^{2+}, Mg^{2+}, Cd^{2+} and X = ClO_4^-, BF_4^-, NO_3^-, indicated several phase transitions below room temperature (principally two) and that the crystal lattice had regular (cubic) symmetry (space group: $Fm\bar{3}m$) in the high temperature phase [1]. The phase transition at T_{C_1}, associated with the largest change of entropy, was associated with a change in the crystal structure (mainly to the monoclinic phase; space group $P2_1/c$) and also with a drastic change in the speed of the reorientational motions of the anions. However, the reorientation of the NH_3 ligands still remain rapid even at the temperature of liquid nitrogen [2–6]. The group of $[M(NH_3)_6](NO_3)_2$ compounds are distinguished particularly by the existence of a large thermal hysteresis of the phase transition at T_{C_2} [1,7]. Hexaamminecobalt(II) nitrate(V) has not yet been investigated from this point of view, so its polymorphism is one of the aims of this study. We also would like to compare the results with those obtained earlier for $[Ni(NH_3)_6](NO_3)_2$, $[Mg(NH_3)_6](NO_3)_2$ and $[Cd(NH_3)_6](NO_3)_2$ [5,6,8–16].

2. Experimental procedure

The initial substance used in the synthesis of the title compound was $[Co(H_2O)_6](NO_3)_2$, which was in turn obtained by a reaction of the corresponding carbonate with diluted HNO_3. The $[Co(H_2O)_6](NO_3)_2$ crystals obtained were re-crystallized several times from double distillated in a quartz vessel water and then dried over BaO. Approximately 12 g of $[Co(H_2O)_6](NO_3)_2$ was added into ca. 80 mL of NH_{3aq} (25%), which had been deoxygenated by a flow of argon. The solution was kept at 333 K for 15 min and then cooled to room temperature. Next, ca. 80 mL of deoxygenated acetone was slowly added by mixing. The resulting precipitate of $[Co(NH_3)_6](NO_3)_2$ was filtered through a glass filter, washed three times with deoxygenated acetone, dried in a stream of argon and then transferred (as a light brown powder) under argon into a tightly sealed vessel. Before measurements were made, the composition of this compound was determined on the basis of its cobalt and ammonia content, using titration by means of EDTA and HCl, respectively. The average content was 20.79% Co^{2+} and 35.72% NH_3 (theoretical values are: 20.67% and 35.84%, respectively). All steps were undertaken in an argon atmosphere (Schlenk apparatus) in order to avoid the oxidation of Co^{2+} to Co^{3+}.

In order to further confirm the identity of the title compound thermal analysis was performed using thermogravimetry using simultaneous differential thermal analysis methods (TGA/DTG/SDTA) by means of a Mettler Toledo TGA/SDTA 851^e

* Corresponding author. Tel.: +48 12 663 2265.
E-mail address: serwonsk@chemia.uj.edu.pl (J. Hetmańczyk).

0040-6031/$ – see front matter © 2009 Published by Elsevier B.V.
doi:10.1016/j.tca.2009.06.017

apparatus. Evolved gaseous products from the decomposition of the compound were identified *on-line* by a quadruple mass spectrometer (QMS) Balzer GSD 300T (more details of this experiment are presented in [17]). A sample of mass equal to 4.6585 mg was placed in an open corundum crucible. The measurements were performed across the temperature range of 300–873 K with a constant flow of argon equal to 100 mL min^{-1} and with a heating scanning rate of 5 K min^{-1}. Temperature was measured by a Pt–Pt/Rh thermocouple with an accuracy of ±0.5 K. The results of this thermal analysis, presented in detail in Section 3.1, taken in addition to the chemical analysis and other information also presented in Section 3.1, fully confirmed the composition of the title compound.

The structural analysis of $[Co(NH_3)_6](NO_3)_2$ was undertaken using the X-ray powder diffraction (XRPD) method. The XRPD data were collected on a Panalytical X'Pert Pro powder diffractometer (operating in Bragg–Brentano geometry). The measurements continued for 2 h only because of the rapid decomposition of the title compound. In order to delay the process of decomposition the sample was prepared as a mixture with paraffin oil. The diffraction pattern was made at an angle of 2θ range of 10–80°. The lattice parameter was defined by Rietveld refinement. The initial model was based on the structure of two similar compounds: $[Co(NH_3)_6](BF_4)_2$ and $[Co(NH_3)_6](PF_6)_2$ [18].

Fourier transform far infrared (FT-FIR) spectrum of $[Co(NH_3)_6](NO_3)_2$ at room temperature was recorded in the wavenumber region 600–50 cm^{-1}, at a resolution of 1 cm^{-1}, on a Nicolet Magna-IR 760 spectrometer equipped with a deuterium triglycyne sulphate (DTGS) detector and a Globar lamp as a light source, for a powdered sample mixed with polystyrene. Fourier transform in middle infrared (FT-MIR) spectra at room temperature was performed with a Bruker EQUINOX 55 spectrometer, in the wavenumber range 4000–400 cm^{-1}, with a resolution of 2 cm^{-1}. Two spectra were made, one for a powdered sample in a KBr pellet and the second for a sample suspended in paraffin oil (Nujol). The FT-MIR measurements of the spectra in the temperature range 290–20 K and the wavenumber range 4000–500 cm^{-1} were carried out for a powdered sample mixed with Nujol and drifted on a KBr pellet. The temperature of the "cold finger" was measured with an accuracy of ±1 K, but the temperature of the sample may have been several Kelvin higher.

UV–vis absorption spectra in an aqueous solution were measured on a Shimadzu 2101PC spectrophotometer. UV–vis reflectance spectra were measured for a sample of the title compound in $BaSO_4$ pellets with $BaSO_4$ as a reference using a Shimadzu 2101 PC spectrometer equipped with an ISR-260 attachment.

Differential scanning calorimetry (DSC) measurements were performed at 93–297 K with a PerkinElmer PYRIS 1 DSC apparatus. The instrument was calibrated using the literature data for indium and water melting points. The enthalpy change (ΔH) was calculated by numerical integration of the DSC curve under the anomaly peak after a linear background arbitrary subtraction. The entropy change (ΔS) was calculated using the formula $\Delta S = \Delta H/T_C$. The powdered sample was placed in an aluminium vessel and closed by compression. The measurements were made both on heating and on cooling a freshly synthesized sample of mass equal to 7.90 mg with constant rates of 10, 20, 30 and 40 K min^{-1}. Other experimental details were the same as those published in [3].

3. Results and discussion

3.1. Spectroscopic (FT-FIR, FT-MIR, UV–vis), structural (XRPD) and thermal (TG, DTG, QMS, SDTA) recognition of the title compound

Fig. 1 shows far and middle infrared (FT-FIR and FT-MIR) spectra for $[Co(NH_3)_6](NO_3)_2$ obtained at room temperature. A factor group

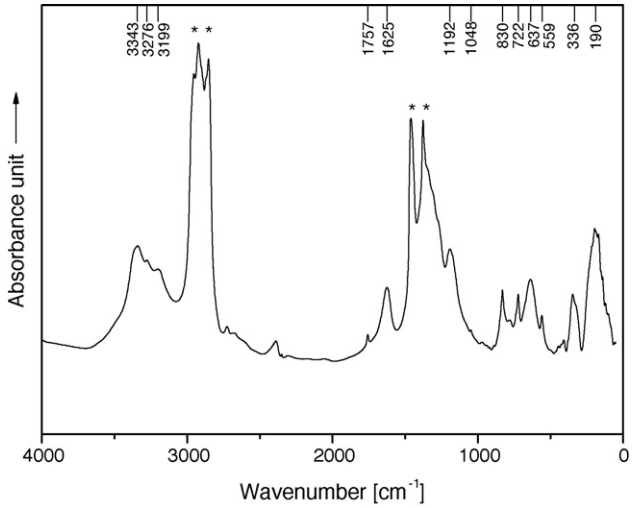

Fig. 1. Infrared spectrum (FT-FIR and FT-MIR) of $[Co(NH_3)_6](NO_3)_2$ at room temperature. Stars denote Nujol bands.

analysis for the $Fm\bar{3}m$ - O_h^5 space group ($Z = 4$) revealed the following 12 lattice vibrations: $F_{1g} + 2F_{1u} + F_{2g}$. However, rotational mode F_{1g} is Raman and infrared inactive [19]. Modes of type u are only infrared active and modes of type g are Raman only active. There are 69 normal vibration modes for the octahedral complex cation of O_h symmetry: $3A_{1g} + A_{1u} + 3E_g + E_u + 4F_{1g} + 7F_{1u} + 4F_{2g} + 4F_{2u}$, but $4F_{1g}$ and A_{1u}, E_u, $4F_{2u}$ are Raman and infrared inactive, respectively. Twelve of them ($F_{1g} + F_{1u} + F_{2g} + F_{2u}$) are connected with the torsions of the NH_3 ligands, but only six modes are Raman (F_{2g}) and infrared (F_{1u}) active [19]. The $Co(NH_3)_6^{2+}$ cation was considered as having octahedral symmetry with nearly freely rotating six ammine ligands. The NO_3^- anion of flat pyramidal D_{3h} symmetry has six normal modes of symmetry: A_1', A_2'' and $2E'$. The first mode ($\nu_1(NO_3^-) = \nu_s(NO)A_1'$) is infrared inactive and the second ($\nu_2(NO_3^-) = \nu_s(NO_3)A_2''$) is Raman inactive. Two modes E', namely: $\nu_3(NO_3^-) = \nu_d(NO)E'$ and $\nu_4(NO_3^-) = \delta_d(ONO)E'$, are active both in the Raman and in the infrared spectrum [20]. Table 1 presents the list of the band positions observed in the FT-FIR plus FT-MIR spectra of $[Co(NH_3)_6](NO_3)_2$, their relative intensities and assignments. For comparison, Table 1 also includes the data obtained for $[Ni(NH_3)_6](NO_3)_2$ [21], $[Mg(NH_3)_6](NO_3)_2$ [5] and $[Cd(NH_3)_6](NO_3)_2$ [5]. These assignments proved that the composition and structure of the investigated compound was correct.

For further verification of the composition of the title compound the UV–vis spectrum was measured. The UV–vis reflectance spectrum of $[Co(NH_3)_6](NO_3)_2$ is presented in Fig. 2a. For comparison, the spectrum of $[Co(NH_3)_6](NO_3)_3$ is also given, both in solution and as a solid (Fig. 2b). $[Co(NH_3)_6](NO_3)_2$ is very unstable in air and oxidizes to $[Co(NH_3)_6](NO_3)_3$. The complex of Co(II) is also very sensitive to moisture and a release of NH_3 is observed. These facts prevent measurement of the spectrum of a solution, also the reflectance spectrum must be measured in restricted conditions, nonetheless traces of Co(III) salt are always visible in the spectrum. The UV–vis spectrum of $[Co(NH_3)_6](NO_3)_3$ in solution in water is dominated by the low intensity (molar extinction coefficients, $\varepsilon < 100$) bands at ca. 476, 341 and 315 nm. The first of these can be attributed to the *d–d* transition from the $^1A_1$ ground state (d^6 configuration). The band positions are almost the same in both the solution and the solid (see Fig. 2b), confirming the *d–d* origin of the bands. The bands in reflectance spectra below 250 nm, both for Co(II) and Co(III) ammine complexes, are in fact the result of Kubelka and Munk [22] transformation, and not real spectral bands. Comparison of the Co(II) and Co(III) complexes spectra indicate that the spectrum of Co(II) is similar to that of Co(III) but in the

Table 1
Infrared band frequencies of the compounds of the type: $[M(NH_3)_6](NO_3)_2$, where M = Co, Cd, Mg and Ni (band intensity: vs – very strong, s – strong, m – medium, w – weak, vw – wery weak, br – broad, sh – shoulder).

Infrared bands frequencies (cm^{-1})				Assignments
This work Co	[5] Cd	[5] Mg	[21] Ni	
3343 s	3395 m,br	3373 s	3346 s	$\nu_{as}(NH)F_{1u}$
3276 s	3278 m,sh	3244 s	3242 sh	$\nu_s(NH)F_{1u}$
3199 s	3208 m,sh	3154 sh		$2\delta_{as}(HNH)F_{1u}$
1757 w	1755 w	1764 w	1764 w	$2\nu_2(NO_3^-)A_2''$
1625 s	1606 s	1632 s	1616 m	$\delta_{as}(HNH)F_{1u}$
*	1456 vs			$2\nu_4(NO_3^-)E'$
*	1381 vs	1385 vs	1383 vs	$\nu_3(NO_3^-)E'$
*	1303 s			
1192 vs	1156 s,br		1192 s	$\delta_s(HNH)F_{1u}$
	1117 s,br			
1048 w,sh	1046 s	1023 m	1045 vw	$\nu_1(NO_3^-)A_1'$
830 s	832 m	826 m	826 m	$\nu_2(NO_3^-)A_2''$
780 w	819 m			$\rho_r(NH_3)F_{1u}$
722 s	721 m			$\nu_4(NO_3^-)E'$
	712 m			$\nu_4(NO_3^-)E'$
637 s	608 s		677 s	$\rho_w(NH_3)F_{1u}$
559 m	563 s	588 s		$\rho_t(NH_3)F_{1u}$
465 w				$\nu_s(CoN)A_{1g}$
		408 m		$\nu_s(MgN)A_{1g}$
			374 w,br	$\nu_s(NiN)A_{1g}$
		367 m		$\nu_{as}(MgN)F_{1u}$
336 w				$\nu_{as}(CoN)F_{1u}$
	334 w			$\nu_s(CdN)A_{1g}$
			327 w	$\nu_{as}(NiN)F_{1u}$
	286 m			$\nu_{as}(CdN)F_{1u}$
			223 m	$\delta_{as}(NNiN)F_{1u}$
190 m				$\delta_{as}(NCoN)F_{1u}$
		180 m,br		$\delta_{as}(NMgN)F_{1u}$
	165 m			$\delta_{as}(NCdN)F_{1u}$
102 w	100 w	98 m	?	$\nu_L(lattice)F_{1u}$
59 w				$\nu_L(lattice)F_{2g}$

* Masked by the bands of Nujol.

300–900 nm range bands can only be seen at 339 and 314 nm. The ground state of Co(II) is ^2E and the first allowed excited state is $^2T_2$ (d^7 configuration). The disappearance of the band at 476 nm is associated with a value of the spectrochemical parameter g (g = 18.2 for Co(III) and g = 9.0 for Co(II)). A g parameter for Co(II) almost twice as low results in a d–d band shift to the near infrared region and

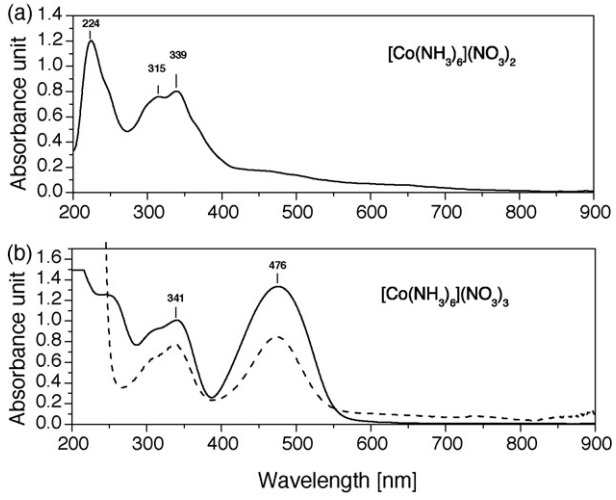

Fig. 2. Room temperature UV–vis spectra of $[Co(NH_3)_6](NO_3)_2$ and $[Co(NH_3)_6](NO_3)_3$ (a) reflectance spectrum of solid $[Co(NH_3)_6](NO_3)_2$; (b) solid line presents reflectance spectrum of solid $[Co(NH_3)_6](NO_3)_3$, dashed line presents aqueous absorption spectrum of $[Co(NH_3)_6](NO_3)_3$ ($c = 1.3 \times 10^{-2}$ M, d = 1 cm). Reflectance spectra are presented after Kubelka–Munk transformation.

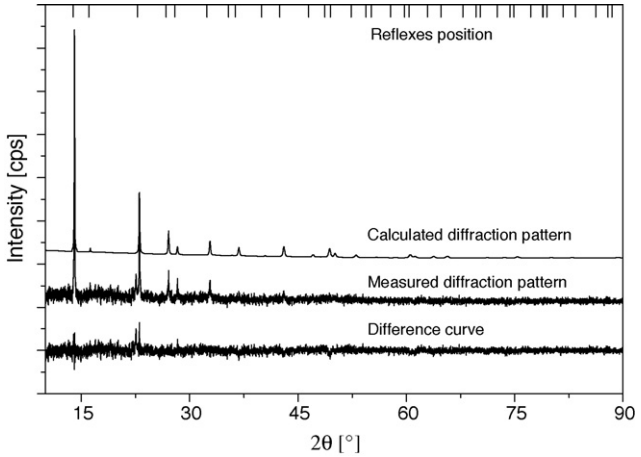

Fig. 3. XRPD diffractogram of $[Co(NH_3)_6](NO_3)_2$ at room temperature.

this band is invisible in the UV–vis spectrum of $[Co(NH_3)_6](NO_3)_2$ presented in Fig. 2.

In order to further confirm the identity of the title compound an X–ray powder diffraction measurement was made. Fig. 3 shows the diffraction pattern of $[Co(NH_3)_6](NO_3)_2$ obtained at room temperature, which can be indexed in a regular system, space group No. 225 = $Fm\bar{3}m = O_h^5$, with the lattice parameter a = 11.0441 Å and with four molecules in the unit cell. The compound has a fluorite type structure, typical for K_2PtCl_6. The structure parameters are very similar to those proposed by Wyckoff [23] for other ionic hexaamminemetal(II) complexes.

Thermal analysis was the next step in the identification of the title compound. Fig. 4 indicates the TG, DTG, SDTA and QMS curves, which show that the thermal decomposition of the investigated compound takes place in two main stages. In stage I four NH_3 ligands per one formula unit of $[Co(NH_3)_6](NO_3)_2$ are evolved in two steps: Ia and Ib, when three NH_3 and one NH_3 molecules per formula unit cleave from the complex cation, respectively. Stage II is connected with the disconnection of the two remaining ligands from the $[Co(NH_3)_2]^{2+}$ cation and with the simultaneous formation of one of the solid cobalt oxides (Co_3O_4, Co_2O_3, CoO) [24]. Formation of the final product of decomposition in the form of Co_3O_4 and/or Co_2O_3 was proposed for $Co(NO_3)_2$ by Ehrhardt et al. [25,26]. However, in our opinion, formation of CoO as well cannot be excluded. The decomposition process of NO_3^- anions begins at stage I (ca. 370 K), which is confirmed by the presence of the minima on QMS curves (see Fig. 4) recorded for the masses (m/z), which were identified as: O_2, and NO_x (NO_2, NO, N_2O). However, the intensification of this process takes place only at stage II (ca. 470 K) and is associated with reduction and oxidation reactions accompanying the $Co^{2+} \leftrightarrow Co^{3+}$ process. These reactions are strongly exothermic, what leads to an increase in the sample temperature and additionally accelerates the decomposition of the NO_3^- anions.

On the SDTA curve (Fig. 4) four endothermic minima and two exothermic maxima are evident. The minima can be explained, also taking into account the results presented above, as being associated with the two-step deammination process in stage I according to the following reactions:

$$\text{Ia}: \quad [Co(NH_3)_6](NO_3)_2 \rightarrow [Co(NH_3)_3](NO_3)_2 + 3NH_3, \qquad (1)$$

$$\text{Ib}: \quad [Co(NH_3)_3](NO_3)_2 \rightarrow [Co(NH_3)_2](NO_3)_2 + NH_3. \qquad (2)$$

Exothermic maxima in stage II are associated with the disconnection of the two remaining NH_3 ligands of $[Co(NH_3)_2](NO_3)_2$ and with the simultaneous decomposition of cobalt nitrate(V) to the oxides of Co(II) and Co(III) together with the nitrogen(IV) and nitro-

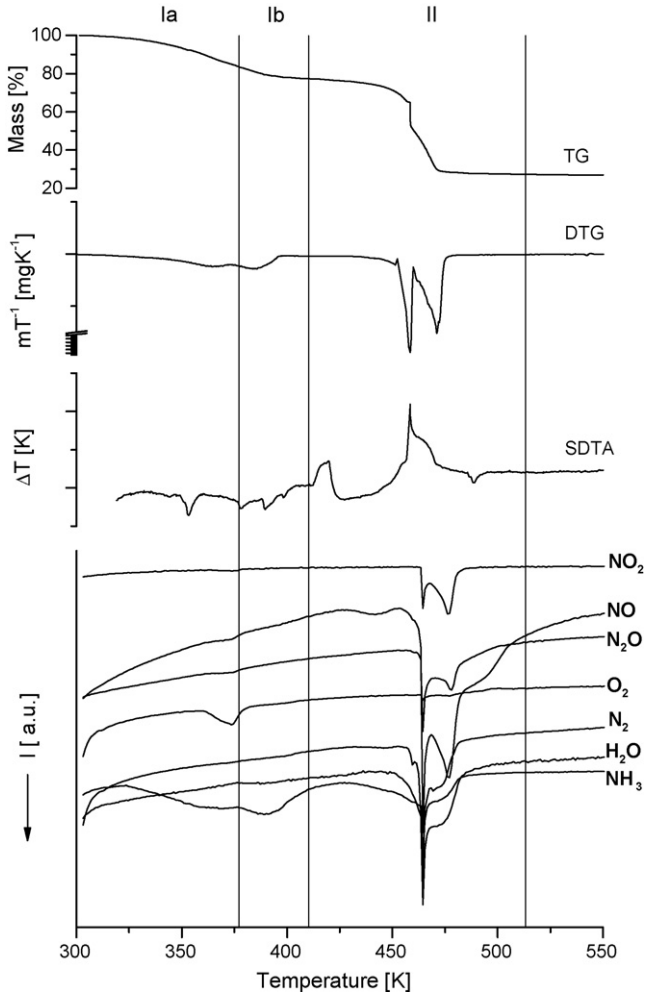

Fig. 4. TG, DTG, SDTA and QMS curves for $[Co(NH_3)_6](NO_3)_2$ at the range of 300–550 K and at a constant heating rate 5 K min^{-1} in a flow of argon.

gen(V) oxides, according to the following hypothetical reactions:

$$\text{II}: \quad [Co(NH_3)_2](NO_3)_2 \rightarrow Co(NO_3)_2 + 2NH_3, \tag{3}$$

$$Co(NO_3)_2 \leftrightarrow (1/2)Co_2O_3 + (1/2)N_2O_4 + (1/2)N_2O_5, \tag{4a}$$

or/and

$$Co(NO_3)_2 \leftrightarrow (1/3)Co_3O_4 + (1/3)N_2O_4 + (2/3)N_2O_5, \tag{4b}$$

or/and

$$Co(NO_3)_2 \leftrightarrow CoO + N_2O_5. \tag{4c}$$

Reactions (4a) and (4b) were proposed by Ehrhardt and coworkers [26]. It was not possible to distinguish which of reactions presented above really take place during $Co(NO_3)_2$ decomposition, because the amount of the solid final product was too small for further analysis.

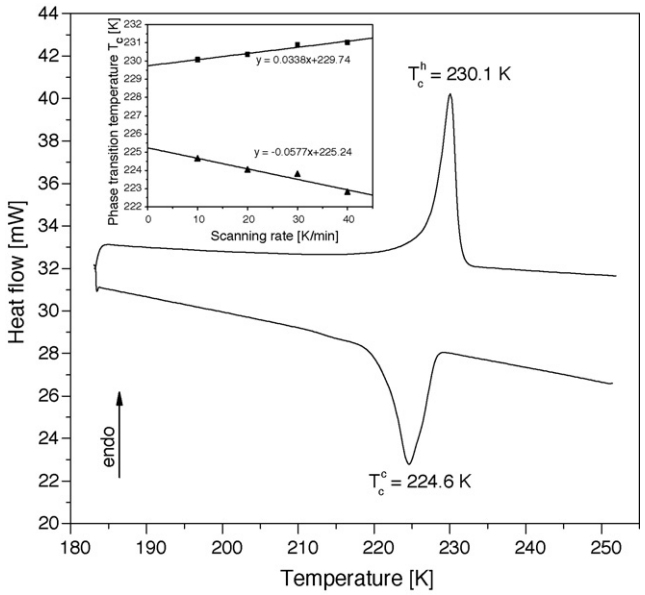

Fig. 5. DSC curves obtained for $[Co(NH_3)_6](NO_3)_2$ at heating and cooling rate of 10 K min^{-1} at the temperature range 185–250 K.

It is also possible that another mechanism of $Co(NO_3)_2$ decomposition and, in consequence, different products from the final reaction can be obtained:

$$Co(NO_3)_2 \leftrightarrow Co(NO_2)_2 + O_2, \tag{4d}$$

$$Co(NO_2)_2 \leftrightarrow CoO + NO + NO_2. \tag{5}$$

It should be pointed out here that the results of thermogravimetric analysis of $[Co(NH_3)_6](NO_3)_2$ presented in this work prefer as solid final product CoO (compare Table 2).

Based on earlier results obtained by us for other metal(II) nitrates(V) [17,27,28] and also on other literature [29], we suggest that the gaseous products may react with each other according, for example, to the following reactions:

$$2NH_3 + 3O_2 + N_2 \leftrightarrow 2NO + N_2O + 3H_2O, \tag{6}$$

and/or

$$2NH_3 + 2.5O_2 \leftrightarrow 2NO + 3H_2O. \tag{7}$$

Of course, it is possible to obtain different products due to temporary concentrations of particular substrates. It is, therefore, very difficult to present proper equations for these reactions. Temperature range, percentage mass loss and products during different stages of the decomposition of $[Co(NH_3)_6](NO_3)_2$ are presented in Table 2.

3.2. Phase transition investigations (DSC)

DSC measurements for $[Co(NH_3)_6](NO_3)_2$ were performed in the temperature range 93–297 K with scanning rates 10, 20, 30

Table 2
Results of the thermal decomposition of $[Co(NH_3)_6](NO_3)_2$ in argon atmosphere with the heating rate of 5 K min^{-1}.

Sample mass [mg]	Stage number	Temperature range [K]	Mass loss at the stage [%]	Mass after decomposition [%]	Calculated values [%]	Products of the decomposition
4.6585	Ia	301–377	16.71		17.92	$3NH_3$
	Ib	378–410	6.31		5.97	$1NH_3$
	II	411–513	50.98	26.00	49.83	$2NH_3 + O_2 + N_yO_x$
	III	Above 514			26.28	CoO
					28.15	Co_3O_4
					29.09	Co_2O_3

Table 3
Thermodynamics parameters of the phase transition obtained during cooling and heating of $[Co(NH_3)_6](NO_3)_2$ extrapolated to the scanning rate equals to 0 K min^{-1}.

Parameters	Cooling	Heating
T_C [K]	225.2 ± 0.1	229.7 ± 0.1
ΔH [kJ mol^{-1}]	4.68 ± 0.16	4.65 ± 0.25
ΔS [J mol^{-1} K^{-1}]	20.90 ± 0.66	20.18 ± 1.02

and 40 K min^{-1} for two different samples of masses: 9.81 mg (sample A) and 9.43 mg (sample B). Fig. 5 presents the temperature dependences of the heat flow (DSC curves) obtained for the title compound on heating (upper curve) and on cooling (lower curve) exemplarily for the sample A, at the rate of 10 K min^{-1}. One distinct anomaly was registered at the scanning rate of 10 K min^{-1} on DSC curves at: $T^h_{peak} = 230.1$ K (on heating) and at: $T^c_{peak} = 224.6$ K (on cooling). The values of phase transition (PT) temperatures: $T^h_C = 229.7$ K and $T^c_C = 225.2$ K were calculated by extrapolating the dependence of the corresponding T^h_{peak} and T^c_{peak} values vs. the scanning rate of heating and cooling the samples to the scanning rate value of 0 K min^{-1}. They correspond well to the *onset* of peaks on corresponding DSC curves. The presence of ca. 4.5 K hysteresis of the PT temperature suggests that the detected phase transition is of the first-order type. The mean values of the PT temperatures, enthalpy and entropy changes of the detected phase transition are presented in Table 3. The entropy change accompanying this PT is equal to about 20 J mol^{-1} K^{-1}, which suggests its "order–disorder" mechanism.

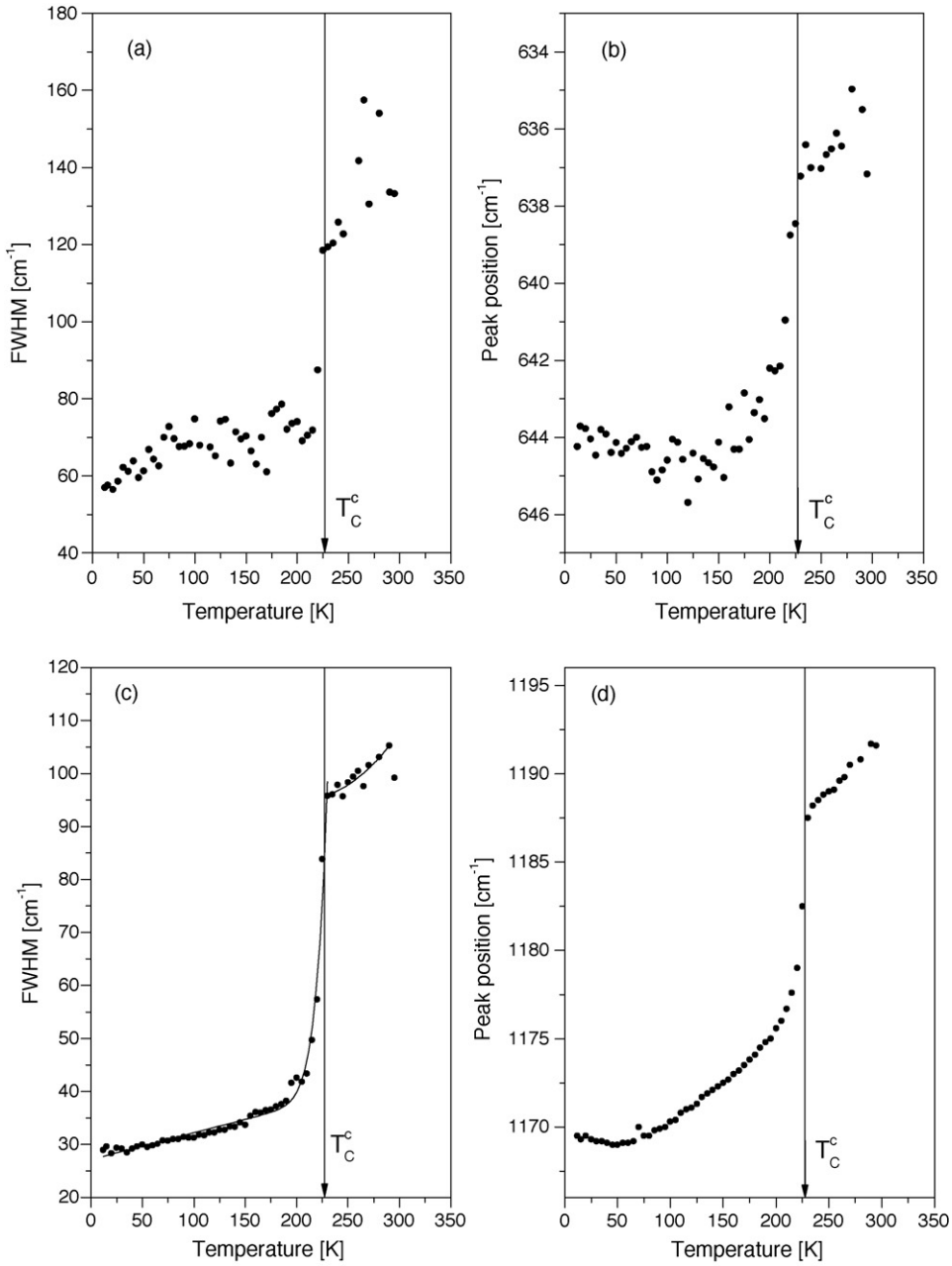

Fig. 6. The temperature dependences: of the infrared band width (FWHM) connected with $\rho_w(NH_3)F_{1u}$ (a) and with $\delta_s(HNH)F_{1u}$ (b) modes. Temperature dependences of these bands wavenumber present (c) and (d), respectively. These dependences were obtained registered infrared spectra at cooling the $[Co(NH_3)_6](NO_3)_2$ sample. Arrows denote temperature T_C of the phase transition (at cooling). Solid lines represent fitting of Eq. (9) to the experimental points.

Table 4
The fitted parameters a, b, c and E_a for the temperature dependence of FWHM of the band at 1192 cm^{-1}, connected with $\delta_s(HNH)F_{1u}$.

Parameters	Band at 1192 cm^{-1} – mode $\delta_s(HNH)F_{1u}$	
	Phase I	Phase II
a [cm^{-1}]	100.00	27.10
b [cm^{-1} K^{-1}]	−0.03	0.05
c [cm^{-1}]	3.61×10^3	7.01×10^{10}
E_a [kJ mol^{-1}]	13.3	39.9

3.3. Molecular motions vs. phase transition (FT-IR bands shape vs. T)

In most of the $[M(NH_3)_6]X_2$ compounds which indicate dynamical orientation disorder of the ammonia molecules [7] the rapid NH_3 reorientation does not stop at the phase transitions [1]. We would like to check if the observed phase transition in the title compound is connected or not with a drastic change of the reorientation dynamics of the NH_3 ligands. We would also like to compare the results with those obtained by us earlier for $[Ni(NH_3)_6](NO_3)_2$ and $[Mg(NH_3)_6](NO_3)_2$ [8–16]. The FT-MIR spectra of $[Co(NH_3)_6](NO_3)_2$ within the wavenumber range 4000–400 cm^{-1} were registered during the cooling of the sample in the temperature range 295–15 K. An analysis of the full with at half maximum (FWHM) for $\rho_w(NH_3)F_{1u}$ and $\delta_s(HNH)F_{1u}$ modes in the infrared spectra vs. temperature was made. We did not performed an analysis of the infrared active $\nu_3(NO_3^-)$ and $\nu_4(NO_3^-)$ modes because theirs FWHMs did not change with temperature. We followed the analysis of FWHM vs. temperature, described by Carabatos-Nédelec and Becker [27,28], which is based on the theory used for the damping associated with an order–disorder mechanism. We assumed that the reorientation correlation time τ_R is the mean time between instantaneous jumps from one potential well to another and it is defined as:

$$\tau_R = \tau_0 \exp\left(\frac{E_a}{RT}\right), \quad (8)$$

where τ_0 is the relaxation time at infinite temperature T, E_a is the height of the potential barrier for reorienting species and R is the gas constant. For vibrations of frequency $\varpi > 1 \times 10^{13}$ s^{-1} and for $\tau_R > 1 \times 10^{-12}$ s, the temperature dependence of the FWHM can be described by [30–32]:

$$\mathrm{FWHM}(T) = (a + bT) + c \exp\left(-\frac{E_a}{RT}\right), \quad (9)$$

where a, b, c and E_a are parameters to fit. The linear part of Eq. (9) corresponds to the bandwidth associated with vibrational relaxation and the exponential term corresponds to the bandwidth associated with the reorientational relaxation.

Fig. 6a and c shows the temperature dependences of the FWHM of the infrared bands associated with the $\rho_w(NH_3)F_{1u}$ and $\delta_s(HNH)F_{1u}$ modes, located at ca. 640 cm^{-1} and 1190 cm^{-1}, respectively. It is evident that during the cooling of the sample the FWHM of these bands decreases exponentially down to the phase transition temperature, where it abruptly and significantly decreases and then continues decreasing exponentially but at a much slower rate. The FWHM values were calculated by fitting the Lorentz function to these two bands for the spectra measured across a wide temperature range (20–300 K) using the Origin program. Unfortunately, we cannot to fit Eq. (9) to the experimental points for the band at ca. 640 cm^{-1} associated with the $\rho_w(NH_3)F_{1u}$ mode because these points are very scattered. In turn it was possible to fit Eq. (9) to the experimental points for the band at ca. 1190 cm^{-1} associated with the $\delta_s(HNH)F_{1u}$ mode and these fit parameters are listed in Table 4. The estimated activation energy values for the rotational motion of the NH_3 ligands are: $E_a(I) = 13.3 \pm 8.6$ kJ mol^{-1} and $E_a(II) = 39.9 \pm 2.7$ kJ mol^{-1}, for the high and low temperature phases respectively. These values are a

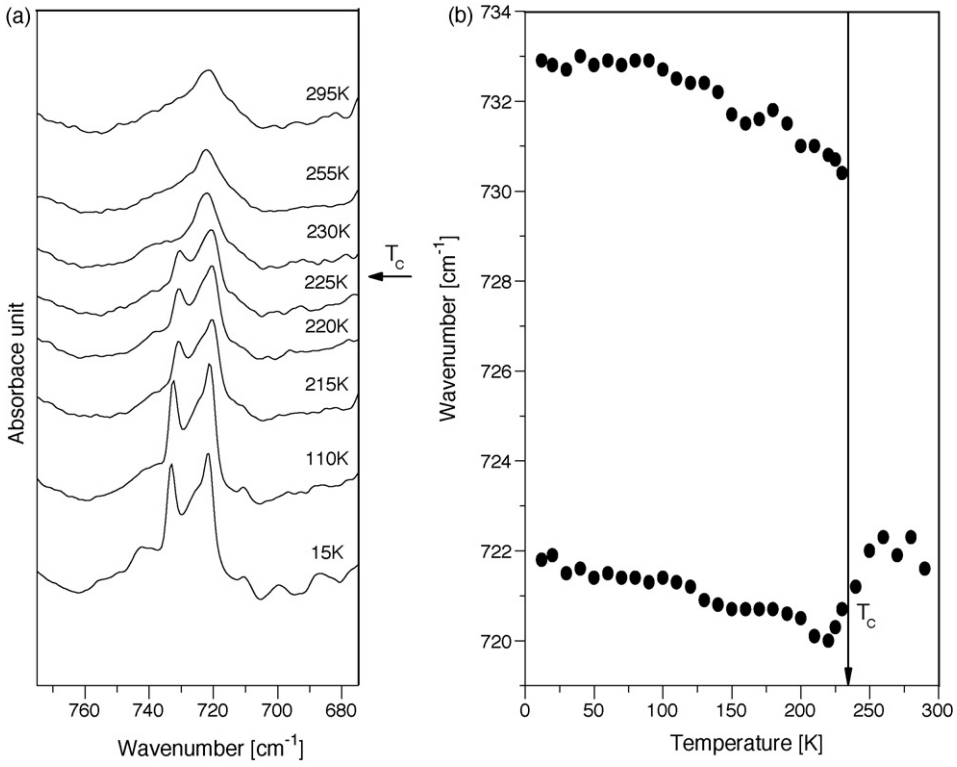

Fig. 7. Temperature dependence of the shape (a) and the position (b) of the band connected with $\nu_4(NO_3^-)E$ mode (at ca. 722 cm^{-1}). Arrow denotes temperature T_C of the phase transition (at cooling).

little higher than those for $Ni(NH_3)_6](NO_3)_2$ (E_a(I) = 4.7 kJ mol^{-1}, E_a(II) = 2.3 kJ mol^{-1}, E_a(III) = 0.1 kJ mol^{-1}, E_a(IV) = 0.5 kJ mol^{-1}) and also for $[Mg(NH_3)_6](NO_3)_2$ (E_a(I) = 7.1 kJ mol^{-1}, E_a(II) = 2.6 kJ mol^{-1}, E_a(III) = 0.1 kJ mol^{-1}, E_a(IV) = 0.6 kJ mol^{-1}) derived from the quasielastic neutron scattering method (QENS) [10–16].

Fig. 6b and d demonstrates the temperature dependence of the band position of the two bands discussed above. We can see that both of these temperature dependences are very similar and, moreover, they are similar to the corresponding FWHM vs. temperature dependences shown in Fig. 6a and c. This fact suggests that the reorientation motions of the NH_3 ligands do contribute to the phase transition mechanism, but that the change of the crystal structure probably plays the dominant role in the phase transition mechanism.

Fig. 7 presents temperature the dependence of the position of the band at ca. 722 cm^{-1} associated with the $\nu_4(NO_3^-)E$ mode. We can see that this band splits below temperature T_C. The splitting of this band suggests that the observed phase transition is related to the symmetry change of the crystal lattice.

4. Conclusions

1. $[Co(NH_3)_6](NO_3)_2$ at room temperature has a regular (cubic) structure, space group No. 225 = $Fm\bar{3}m = O_h^5$, with the lattice parameter a = 11.0441 Å and with four molecules in the unit cell.
2. The DSC measurements of $[Co(NH_3)_6](NO_3)_2$ performed in the temperature range 90–297 K allowed one phase transition to be detected. The value of temperature of the phase transition obtained by extrapolating the values obtained at different scanning rates to the zero scanning rate amounts to: $T_C^h = 229.7$ K and $T_C^c = 225.2$ K, respectively. The presence of 4.5 K hysteresis suggests that the detected PT is of the first-order type. The entropy change accompanying this PT suggests its "order–disorder" mechanism.
3. The temperature dependences of the FWHM of the band associated with the $\delta_s(HNH)F_{1u}$ mode indicates fast reorientation of the NH_3 ligands with reorientational correlation times in the order of picoseconds and with an activation energy of E_a(I) = 13.3 ± 8.6 kJ mol^{-1} and E_a(II) = 39.9 ± 2.7 kJ mol^{-1}, for the high and low temperature phase, respectively. The sudden change of FWHM vs. T dependence at T_C suggests that the observed PT is connected with a sudden change in the speed of the NH_3 reorientational motions.
4. The characteristic changes in the band frequencies in the FT-MIR spectra are convincingly observed. The splitting of the band at ca. 722 cm^{-1} connected with the $\nu_4(NO_3^-)E$ mode near temperature T_C suggests that the observed phase transition is probably connected with the change of the site symmetry of the anion. So, the observed PT probably has a structural character.
5. Thermal decomposition of the title compound proceeded in two main stages. In the first stage, deammination of $[Co(NH_3)_6](NO_3)_2$ to $[Co(NH_3)_2](NO_3)_2$ is undergone in two steps and four out of six NH_3 molecules per formula unit are liberated. The second stage is connected with the liberation of the two residual NH_3 molecules and with the simultaneous decomposition of the resulting cobalt(II) nitrate(V), next leading to the formation of the gaseous products of the decomposition (N_2, O_2, H_2O, nitrogen oxides) and solid CoO.

Acknowledgements

We are very grateful to Professor St. Wróbel, PhD, DSc, from the Faculty of Physics, Astronomy and Applied Computer Science of the Jagiellonian University for enables us to perform DSC measurements. Our thanks are also due to J. Chruściel, PhD, DSc, from Faculty of Science of the Podlaska Academy in Siedlce for registering the FT-FIR spectrum of our sample.

References

[1] J.M. Janik, J.A. Janik, A. Migdał-Mikuli, E. Mikuli, K. Otnes, Physica B 168 (1991) 45.
[2] E. Mikuli, A. Migdał-Mikuli, J. Mayer, J. Therm. Anal. 54 (1998) 93.
[3] E. Mikuli, A. Migdał-Mikuli, S. Wróbel, Z. Naturforsch. 54a (1999) 225.
[4] A. Migdał-Mikuli, E. Mikuli, S. Wróbel, Ł. Hetmańczyk, Z. Naturforsch. 54a (1999) 590.
[5] A. Migdał-Mikuli, M. Liszka-Skoczylas, E. Mikuli, Phase Transit. 80 (2007) 547.
[6] M. Liszka-Skoczylas, E. Mikuli, Na pograniczu chemii i biologii, vol. XVI, WN UAM, Poznań, 2006, pp. 151–159 (in polish).
[7] P. Shiebel, W. Prandl, Z. Phys. B 104 (1997) 137.
[8] A. Migdał-Mikuli, E. Mikuli, Acta Phys. Polon. A 88 (1995) 527.
[9] J.M. Janik, J.A. Janik, R.M. Pick, M. le Postollec, J. Raman Spectrosc. 18 (1987) 493.
[10] J.A. Janik, J.M. Janik, A. Migdał-Mikuli, E. Mikuli, T. Stanek, J. Mol. Struct. 115 (1984) 5.
[11] A. Belushkin, J.A. Janik, J.M. Janik, I. Natkaniec, W. Nawrocik, W. Olejarczyk, K. Notes, T. Zaleski, Physica B 122 (1985) 217.
[12] A.W. Belushkin, J.A. Janik, J.M. Janik, I. Natkaniec, K. Otnes, Physica B 128 (1985) 289.
[13] G.J. Kearley, H. Blank, Can. J. Chem. 66 (1988) 692.
[14] J.A. Janik, J.M. Janik, A. Migdał-Mikuli, E. Mikuli, K. Otnes, Physica B 111 (1981) 62.
[15] J.A. Janik, J.M. Janik, A. Migdał-Mikuli, E. Mikuli, M. Rachwalska, T. Stanek, K. Otnes, B.O. Fimland, I. Svare, Physica B 122 (1983) 315.
[16] A. Belushkin, J.A. Janik, J.M. Janik, B. Janik, A. Migdał-Mikuli, E. Mikuli, I. Natkaniec, J. Wąsicki, Physica B 128 (1985) 292.
[17] E. Mikuli, M. Liszka, M. Molenda, J. Therm. Anal. Calorim. 89 (2007) 573.
[18] S. Kummer, D. Babel, Z. Naturforsch. B 39 (1984) 1118.
[19] K.H. Schmidt, A. Müller, Coordin. Chem. Rev. 19 (1976) 41.
[20] K. Nakamoto, Infrared and Raman Spectra of Inorganic and Coordination Compounds, Hardcover, 1997.
[21] T.E. Jenkins, L.T.H. Ferris, A.R. Bates, R.D. Gillard, J. Phys. C: Solid State Phys. 11 (1978) L77.
[22] P. Kubelka, F. Munk, Z. Tekn. Phys. 12 (1931) 593.
[23] R.W.G. Wyckoff, Crystal Structures, vol. 3, Interscience, New York, 1965.
[24] W.W. Wendlandt, J.P. Smith, J. Inorg. Nucl. Chem. 25 (1963) 985.
[25] C. Ehrhardt, M. Gjikaj, W. Brockner, Thermochim. Acta 432 (2005) 36.
[26] W. Brockner, C. Ehrhardt, M. Gjikaj, Thermochim. Acta 456 (2007) 64.
[27] A. Migdał-Mikuli, E. Mikuli, R. Dziembaj, D. Majda, Ł. Hetmańczyk, Thermochim. Acta 419 (2004) 223.
[28] A. Migdał-Mikuli, J. Hetmańczyk, Ł. Hetmańczyk, J. Thermal. Anal. Calorim. 89 (2007) 499.
[29] B. Małecka, Rozprawy i Monografie, vol. 144, UWND AGH, Kraków, 2005 (in polish).
[30] C. Carabatos-Nédelec, P. Becker, J. Raman Spectrosc. 28 (1997) 663.
[31] P. da, R. Andrade, A.D. Pasad Rao, R.S. Katiyar, S.P.S. Porto, Solid State Commun. 12 (1973) 847.
[32] G. Bator, R. Jakubas, J. Baran, Vib. Spectrosc. 25 (2001) 101.